physica status solidi a

phys. stat. sol. (a) **202**, No. 14, 2742–2752 (2005) / **DOI** 10.1002/pssa.200521045

Characterization of a new transparent-conducting material of ZnO doped ITO thin films

H. M. Ali*

Physics Department, Faculty of Science, South Valley University, 82524 Sohag, Egypt

Received 1 June 2005, revised 11 September 2005, accepted 21 September 2005
Published online 4 November 2005

PACS 61.10.Nz, 68.55.Jk, 73.61.Le, 78.20.Ci, 78.66.Li

Thin films of indium tin oxide (ITO) doped with zinc oxide have the remarkable properties of being conductive yet still highly transparent in the visible and near-IR spectral ranges. The Electron beam deposition technique is one of the simplest and least expensive ways of preparing. High-quality ITO thin films have been deposited on glass substrates by Electron beam evaporation technique. The effect of doping and substrate deposition temperature was found to have a significant effect on the structure, electrical and optical properties of ZnO doped ITO films. The average optical transmittance has been increased with increasing the substrate temperature. The maximum value of transmittance is greater than 84% in the visible region and 85% in the NIR region obtained for film with Zn/ITO = 0.13 at substrate temperature 200 °C. The dielectric constant, average excitation energy for electronic transitions (E_o), the dispersion energy (E_d), the long wavelength refractive index (n_∞), average oscillator wave length (λ_o) and oscillator strength S_o for the thin films were determined and presented in this work.

1 Introduction

Transparent conducting oxides (TCOs) possess low resistivity, exhibit good adherence to many substrates, and have good transmission characteristics from the visible to near-infrared wavelengths, which make it useful for various applications. These transparent, metallic oxides include, in part, indium-oxide, tin-oxide, indium-tin-oxide, zinc-oxide, cadmium–indium-oxide and cadmium-tin-oxide. These TCOs are used in a variety of applications including: solar cells [1]; liquid crystal displays [2]; anti-static coatings on instrument panels [3]; corrosion resistant coatings [4]; gas sensors [5]; ohmic contacts to surface-emitting lasers [6]; ohmics contacts to light emitting diodes [7]; ohmic contacts to photodetectors [8]; Schottky contacts to photodetectors [9]; and heat mirrors for energy efficient windows and light bulbs [10]. The properties of these films are highly dependent on the defect structures, method of deposition, substrate temperature and film thickness.

ZnO is normally an n-type semiconductor with a room temperature band gap of 3.2 eV [1]. While stoichiometric ZnO films are highly resistive, highly conducting films can be made by creating oxygen vacancies, which act as donors.

Indium tin oxide films (ITO) have been studied for many years and several applications have been found. Different deposition techniques of films have been reported, such as reactive thermal evaporation [11], spray pyrolysis [12], rf-sputtering [13] and electron beam evaporation [14]. Transparency and conductivity of this highly degenerate and wide band gap oxide semiconductor film can be varied by adjusting the dopant material and substrate temperature during the deposition.

* e-mail: hazem95@yahoo.com

In a previous paper [15] we studied the effect of thickness and the post deposition treatment parameters on the ITO optical and electrical properties, demonstrating that the thickness values were very important for calculations of the electrical resistivity and the post deposition treatment were very important for enhancing both the optical and electrical properties of ITO films.

Advancement of TCO's may not only lay within the improvement of existing materials in use (such as SnO_2, ITO, ZnO, etc.), but also the development of novel materials. In the present work, the study of the ZnO doping effect and substrate temperature on the optical and electrical properties of indium tin oxide (ITO) thin films deposited by electron beam evaporation technique was made and the results are reported here and discussed.

2 Experimental

In the present investigation ITO films were prepared from a highly pure (99.999%) cold pressed powder of 90 wt% In_2O_3 and 10 wt% SnO_2 as described in [15]. Thin films of ZnO doped ITO (Zn/ITO = 0, 0.13, 0.31 and 0.55) with thickness of 170 nm were grown onto ultrasonically cleaned glass substrates, using electron beam evaporation technique from a highly pure (5*N*) cold pressed powder of In_2O_3–SnO_2 and ZnO grinded separately and sieved. In order to increase the diffusion process and consequently improve the homogeneity of the material, the tablets were heated up to 900 °C for 3 h.

The glass substrates have been ultrasonically cleaned by means of ultrasonic cleaner instrument model (T-9) using both acetone and carbon tetrachloride as solvents for 2 h and 1 h, respectively. Then, it has been well washed by distilled water and left to dry in a muffle over at 100 °C.

Thin films of the prepared tablet were deposited using Edwards high vacuum coating unit model E306A. The evaporation conditions were: (1) a vacuum of 2×10^{-5} Torr; (2) an accelerating voltage of 3 kV; (3) electron beam current 8–14 mA; and (4) the substrate temperature during deposition was maintained at room temperature, 100, 150 and 200 °C. The rate of evaporation was controlled within the range 10–15 nm/min. The film thickness and deposition rate were controlled by means of a digital film thickness monitor model TM200 Maxtek. Investigations of the microstructure was carried out on Phillips (PW-1710) Cu diffractometer XRD (λ = 1.541838 Å) by varying diffraction angle 2θ from 4 to 70 by step width of 0.04 in order to evaluate crystalline phase and crystallite orientation.

The surface morphology of thin films was performed by using a metallurgical microscope type (Inverted metallurgical microscope Epiphot 300). This microscope is attached with video camera (DSP color camera) and PIV computer.

Optical transmittance (T) and reflectance (R) were measured over the wavelength range 200–2500 nm by using a Jasco V-570 UV-visible-NIR spectrophotometer with a scan speed of 1000 nm/min. Spectra were recorded at room temperature. The transmittance and reflectance data were used to calculate absorption coefficient of the films at different wavelengths. The absorption coefficient, α, is given by the relation:

$$\alpha = \frac{2.303}{d} \log_{10}\left(\frac{1-R}{T}\right), \tag{1}$$

where d is the film thickness.

The refractive index can be determined from the following relation:

$$n = \frac{1+R}{1-R} \pm \left[\left(\frac{R+1}{R-1}\right)^2 - \left(1+k^2\right)\right]^{1/2}, \tag{2}$$

where $k = \alpha\lambda/4\pi$ is the extinction coefficient. In the present work, more reasonable values for n may be determined by considering the plus sign of Eq. (2).

The real dielectric constant ε', which is resulted due to the contribution from the free carrier electric susceptibility, can be written by the following relation [16]:

$$\varepsilon' = n^2 - k^2 = \varepsilon_i - e^2/\pi c^2 (N/m^*)\, \lambda^2 , \tag{3}$$

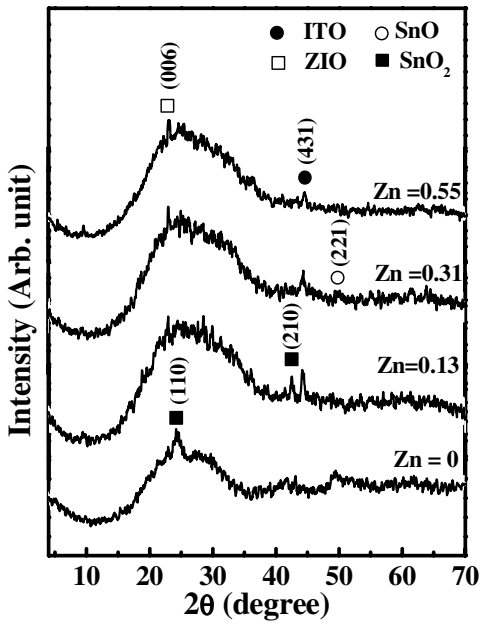

Fig. 1 X-ray diffraction patterns for undoped and ZnO doped ITO thin films (d = 170 nm).

where ε_i is the infinitely high frequency dielectric constant or the residual dielectric constant due to the ion core, N/m^* is the ratio of carrier concentration to the effective mass. Thus, using the previous equations, α, k, n, ε_i and N can be determined from transmission and reflectance measurements.

The film resistivity measurements were carried out at room temperature using a Keithley 614 electrometer with simple two-probe contacts separated by 2 mm.

3 Results and discussion

Figure 1 shows the X-ray diffraction patterns of undoped and ZnO doped ITO films. It is clear that, all films seem to be amorphous. Small peaks corresponding to SnO, SnO_2, ITO and $Zn_2In_2O_5$ (ZIO) are embedded in the amorphous matrix of ZnO doped ITO. The relative intensity of these peaks was noted to change with increasing of ZnO doping. It is observable from this figure that, the intensity of ITO (431) peak decreased with increasing the ZnO doping. This suggests that some of Sn^{4+} ions are substituted by Zn^{2+}. The reason that Zn^{2+} replaced the Sn^{4+} atoms and did not replace the In^{3+} atoms can be interpreted as, that the ionic radius of Sn^{4+} (0.71Å) is very close to that of the ionic radius of Zn^{2+} (0.74 Å), whereas the ionic radius of In^{3+} equal to 0.81 Å. So it is easy that the Zn^{+2} atoms substitute the Sn^{4+} atoms about the In^{3+} atoms.

Figure 2 shows the surface morphology of undoped and ZnO doped ITO films deposited at room temperature. It is evident that, the surface of undoped film seems to be smooth and contains few small grains confirming the nearly amorphous nature of the film. For ZnO doped ITO it is observed that, the excess of ZnO incorporation seems to have influenced on the surface morphology of the ITO, as increasing the ZnO ratio the number of grains increase. For films having Zn/ITO = 0.31 and 0.55, more grains could be observed in the amorphous matrix and may be attributed to the new phase formed due to the ZnO addition.

Measurements of spectral transmittance and reflectance of the sample showed that the films transparency all over the spectral range 200–2500 nm of all the ITO films doped with ZnO were higher than those of the undoped one as shown in Fig. 3. The films appeared brownish in color and exhibited an optical transparency less than 50%. It was observed also that the film transparency initially increased and after that decreased with increasing ZnO doping (Fig. 3(a)). This is may be due to the oxygen vacancies or the behavior of free carriers concentration with increasing the ZnO doping, illustrated in Fig. 4.

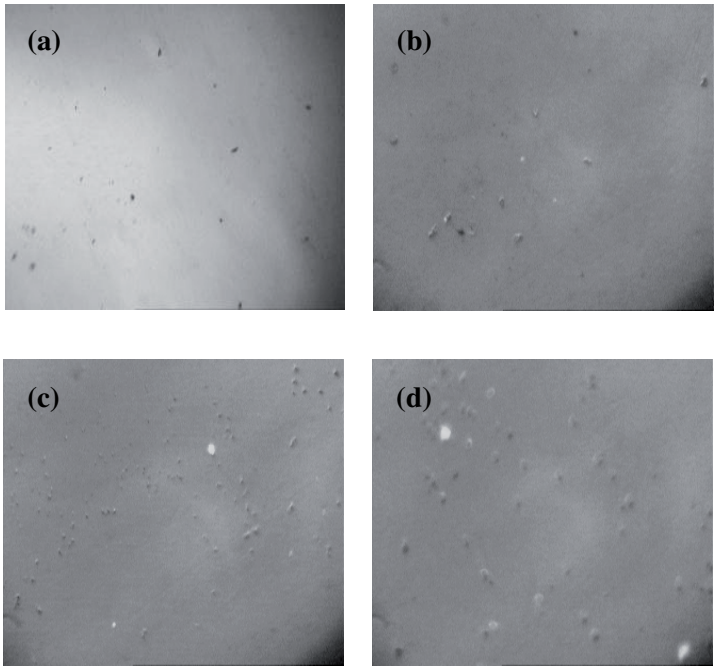

Fig. 2 Surface morphology of undoped (a) and ZnO doped ITO films having ZnO/ITO = 0.13 (b), 0.31 (c) and 0.55 (d) deposited at room temperature.

As it is known, increasing the oxygen vacancies lead to increase the carrier concentration which degrade the transparency due to free-carrier absorption [17]. It is clear also that the absorption edge generally lies in the visible region for ZnO doped ITO.

We have used Drude's theory of dielectrics to obtain the values of carrier concentration N and mobility carrier μ from the optical data. The variations in carrier concentration N, mobility carriers μ, and resistivity ρ with the ratio of ZnO to ITO films are shown in Fig. 4. Undoped ITO film prepared by vacuum evaporation is degenerate semiconductors. Typically with a carrier concentration N which is in the range 1.6×10^{21} cm^{-3}. The mobility carrier is 0.2 cm^2/Vs, and a resistivity ρ is 2×10^{-2} Ω cm. In the case of ZnO doped ITO films, the carrier concentration in the range of $3.8 \times 10^{20} - 8.8 \times 10^{20}$ cm^{-3}. The mobility carrier is 0.4–0.7 cm^2/Vs, and the electrical resistivity is $1.1 \times 10^{-2} - 2.2 \times 10^{-2}$ Ω cm. It is obvious in

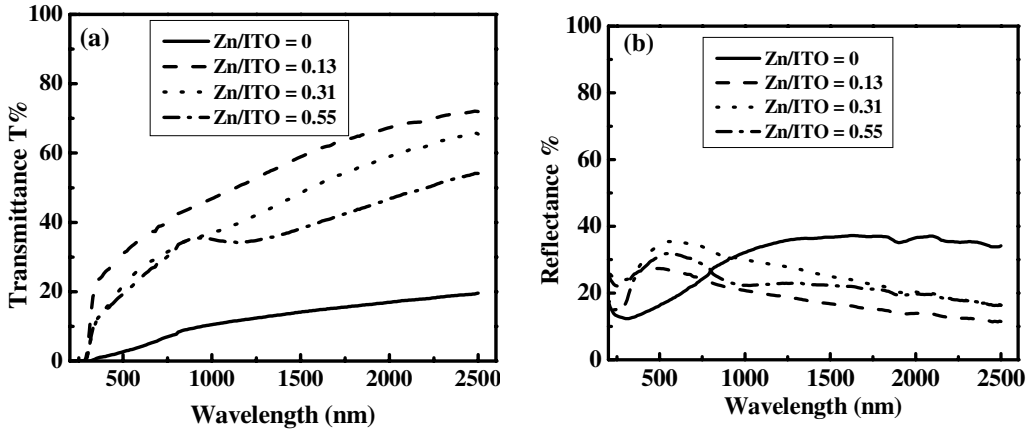

Fig. 3 Spectra of transmittance (a) and reflectance (b) of undoped and ZnO doped ITO thin films.

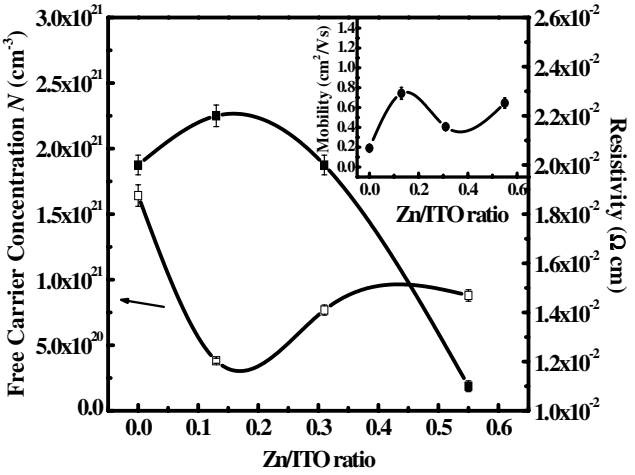

Fig. 4 Variation of the electrical resistivity and carrier concentration for as-deposited ZnO doped ITO thin films at room temperature. In the inset variation of mobility carrier with Zn/ITO ratio is shown.

Fig. 4 that, the resistivity initially increased, which can be attributed to the disorder in the material as a result of doping effect and after that the resistivity decreased quickly with increasing ZnO concentration reaching a minimum of $1.1 \times 10^{-2}\ \Omega$ cm for Zn/ITO = 0.55, so we can conclude that, the resistivity is directly related to the charge carrier concentration of the material in the Drude model [18]. The relatively high resistivity for the films may be due to relatively poor crystallinity of these films. The initial decrease of carrier concentration can be interpreted in terms of the carrier compensation due to doped Zn, acting as an acceptor. The increase of carrier concentration with increasing the ZnO is related to the formation of ternary compound $Zn_2In_2O_5$, as seen in Fig. 1 (XRD patterns)

A usual method of estimating band gap is to plot the graphs of $(\alpha h\nu)^{1/r}$ versus $h\nu$ for various values of r. Where, α is the absorption coefficient, $h\nu$ is the photon energy, r is an exponent that depends upon the type of transitions involved. For allowed transitions, $(\alpha h\nu)^{1/r}$ depends linearly on $h\nu$ above E_g so that extrapolation of straight line portion of the plot (at $h\nu > E_g$) to zero absorption value gives magnitude of energy gap. In the present study, Fig. 5(a) suggests a progressive reduction of the band gap of ZnO-doped ITO films with increasing the ZnO doping, and that a tentative extrapolation of the band gap has been attempted in Fig. 5(a), whose results are plotted in Fig. 5(b), despite the small linear region shown in the absorption spectra above the band gap for the doped samples. It is clear that the variation of $(\alpha h\nu)^2$ versus

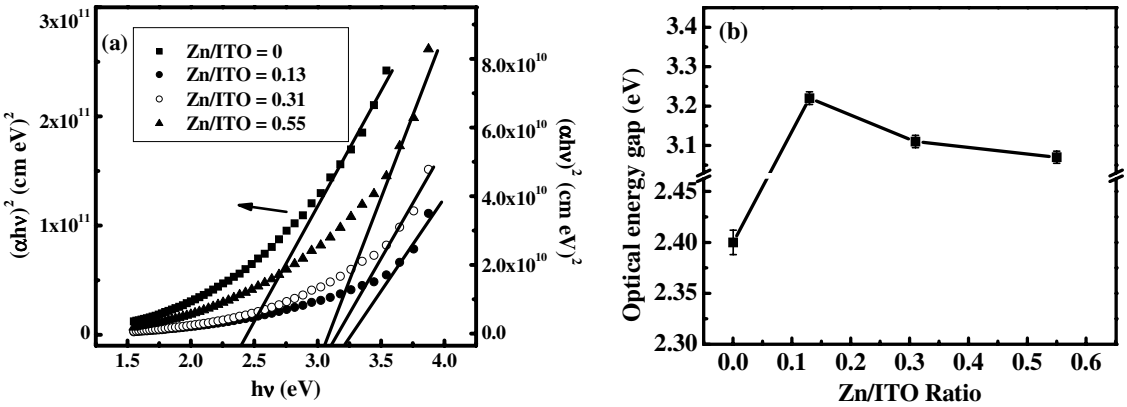

Fig. 5 Plot of $(\alpha h\nu)^2$ vs. $h\nu$ (a) and plot of the optical band gap E_g (b) for undoped and ZnO doped ITO thin films.

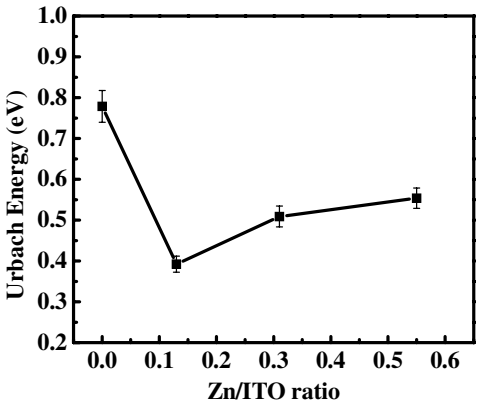

Fig. 6 Plot of Urbach energy as a function of Zn/ITO ratio.

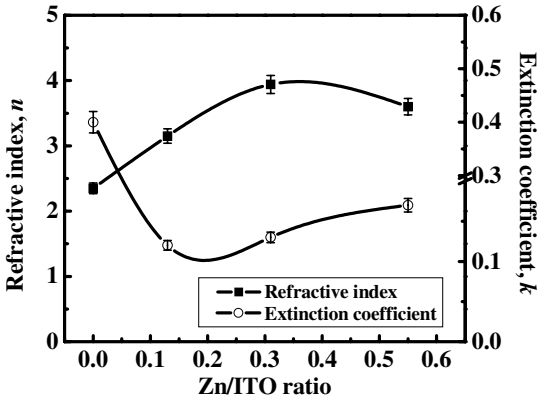

Fig. 7 Variations of the refractive index (n) and extinction coefficient (k) in the visible region with Zn/ITO ratio.

$h\nu$, which is straight line, indicating the presence of direct optical transition. The decrease of the energy band gap can be, in general, correlated with the creation of new donor levels in forbidden zone.

The absorption edge can be determined from the exponential dependence of the absorption coefficient and it is determined as [19],

$$\alpha(h\nu) = \alpha_o \exp(h\nu/E_u), \tag{4}$$

where α_o is a constant and E_u is the Urbach energy which is interpreted as the width of tails of localized states in the gap region. Plotting the dependence of ln α vs. $h\nu$ should give a straight line. The E_u values were calculated from the following relationship, $E_u = (d \ln \alpha / \mathrm{d}\, h\nu)^{-1}$ as shown in Fig. 6. It is observable that, the Urbach energy suddenly decreased at Zn/ITO = 0.13 and after that increased gradually with increasing the ZnO ratio, this may be due to that, ZnO doping causes a shift in the optical absorption edge therefore change in the band structure of the films. Increasing the optical absorption edge of the films with increasing the ZnO ratio indicate that, the dopant ratio is responsible for the width of localized states in the optical band of the films and causes an increase in the energy width of localized states thereby reducing the optical energy gap.

Figure 7 shows the variation of refractive index and extinction coefficient in the visible region with Zn/ITO ratio. It has been noticed that the extinction coefficient decreased from 0.4 for undoped ITO to 0.12 for Zn/ITO = 0.13 films and after that increased slightly with increasing the ZnO doping; this is due to the increase of absorption with increasing the doping. The ZnO-doping also affects the refractive index of the films as shown in Fig. 7. The refractive index is observed to increase from 2.35 to 3.94 with an increase in ZnO/ITO ratio from 0 to 0.31 and then slightly decreased at Zn/ITO = 0.55.

The refractive index dispersion for crystalline and amorphous materials can be expressed as [20],

$$\left(n^2 - 1\right)^{-1} = \frac{E_o}{E_d} - \frac{1}{E_o E_d}(h\nu)^2, \tag{5}$$

where n is the refractive index, h is Planck's constant, ν is the frequency, $h\nu$ is the photon energy, E_o (single oscillator energy) is the average excitation energy for electronic transitions and E_d is the dispersion energy, which is a measure of the strength of interband optical transitions. By plotting $(n^2 - 1)^{-1}$ against $(h\nu)^2$ and fitting a straight line, E_d and E_o can be determined directly from the slope $(E_d E_o)^{-1}$ and the intercept E_o/E_d on the vertical axis. Values of E_o and E_d are shown in Fig. 8. It was observed that the values of E_o initially increased and after that decreased with increasing the ZnO content, this may be due

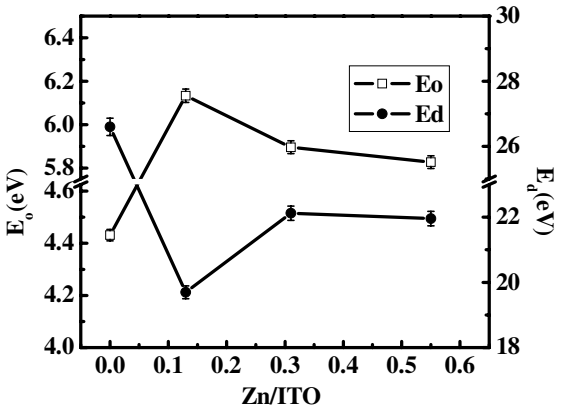

Fig. 8 Plot of the single oscillator energy (E_o) and the dispersion energy (E_d) as a function of Zn/ITO ratio.

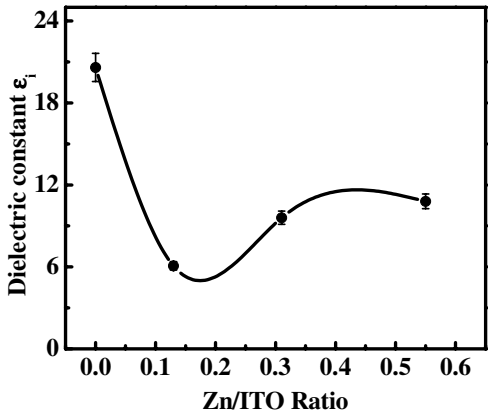

Fig. 9 Variation of the high frequency dielectric constant (ε_i) with the Zn/ITO ratio.

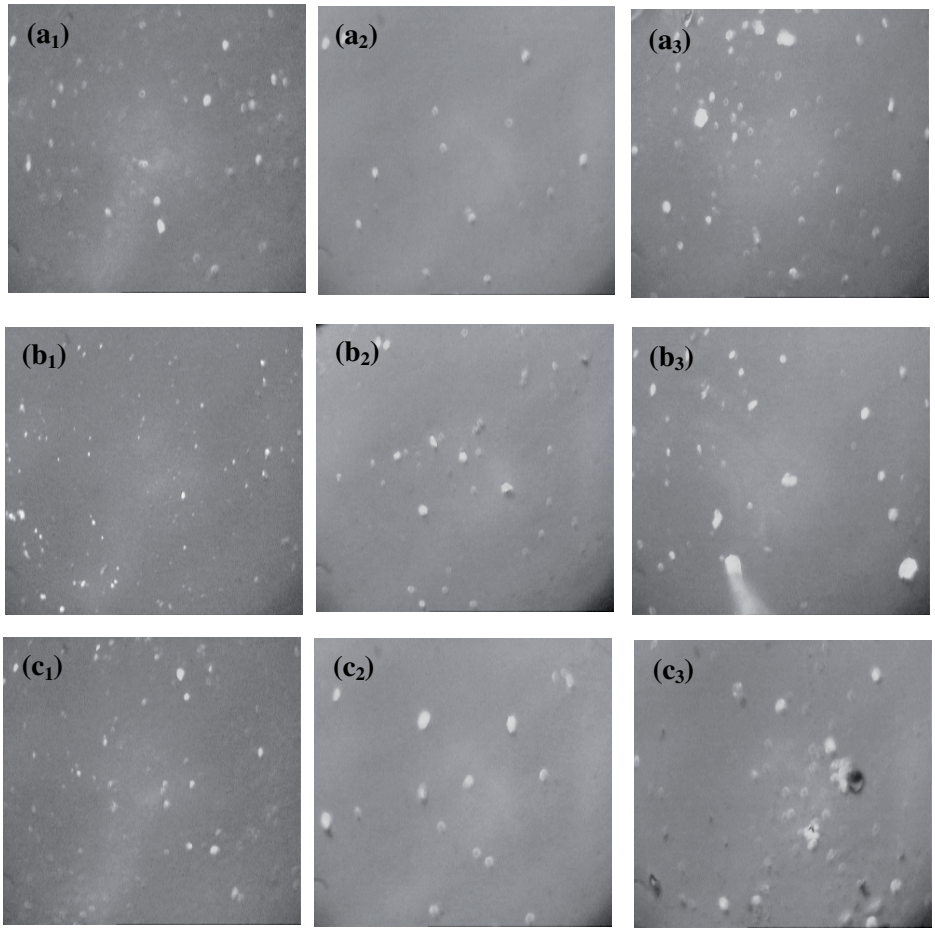

Fig. 10 Surface morphology of ZnO/ITO = 0.13 (a_1, a_2, a_3), 0.31 (b_1, b_2, b_3) and 0.55 (c_1, c_2, c_3) thin films at substrate temperatures 100, 150 and 200 °C, respectively, for each composition.

Table 1 Some optical and electrical properties of ZnO doped ITO deposited at different substrate temperatures (λ_{cutoff} is the short-wave cutoff wavelength, ρ is the film resistivity, μ is the carrier mobility, N is the free carrier concentration, ε_∞ is the infinitely high frequency dielectric constant, n_{550} is the refractive index (at 550 nm of wavelength), n_∞ is the long wavelength refractive index, E_o is the average excitation energy for electronic transitions, E_d is the dispersion energy, S_o is the oscillator strength and λ_o is the average oscillator wave length).

	Zn/ITO = 0.13			Zn/ITO = 0.31			Zn/ITO = 0.55		
	100 [°C]	150 [°C]	200 [°C]	100 [°C]	150 [°C]	200 [°C]	100 [°C]	150 [°C]	200 [°C]
λ_{cutoff} [μm]	0.339	0.335	0.329	0.344	0.339	0.335	0.375	0.370	0.364
$10^{-3}\ \rho$ [Ω cm]	12	9.89	8.25	7.01	6.23	4.20	6.60	4.32	2.12
μ [cm^2/Vs]	4.56	1.88	1.63	1.7	1.56	2.15	1.35	1.74	3.52
$10^{20}\ N$ [cm^{-3}]	1.14	3.36	4.63	5.23	6.42	6.93	7.01	8.32	8.38
ε_i	3.31	3.32	3.78	3.25	3.77	4.35	3.32	3.98	4.61
n_{550}	2.49	2.28	2.25	2.57	2.35	2.39	2.88	2.59	2.22
n_∞	2.16	2	1.99	2.74	2.47	2.16	3.86	3.29	2.02
E_o [eV]	5.19	5.55	5.88	3.93	4.16	5.69	3.77	3.97	5.73
E_d [eV]	5.56	5.23	5.53	4.58	4.25	5.5	4.49	4.16	5.44
$10^9\ S_o$ [m^{-2}]	3.93	3.43	2.97	13	11.4	4.17	5.37	4.7	4
λ_o [nm]	304.8	296.1	315.9	223.3	211.8	296.7	509.2	458.	278.6

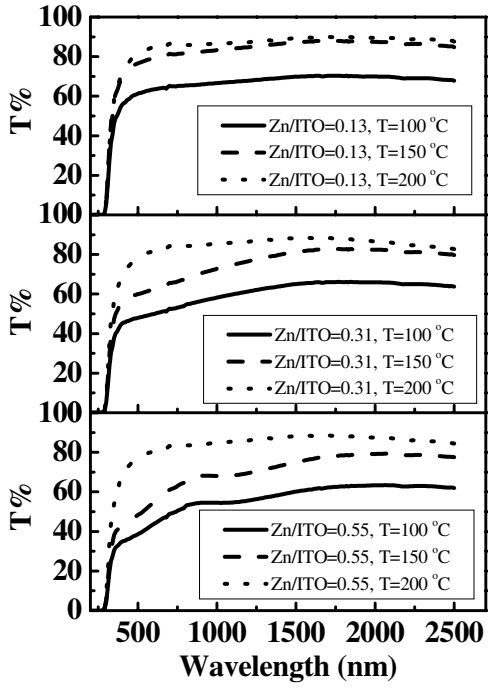

Fig. 11 Spectral variation of the transmittance T with wavelength for ZnO doped ITO thin films at different substrate temperatures.

to the behavior of the optical energy gap. There is a direct relation between E_g and E_o [21]. Hence, a decrease in E_g (darkening) must be accompanied by a decrease in E_o.

The high frequency dielectric constant was determined from the spectral dependences of n and k in the IR region using Eq. (3). Figure 9 shows the variations of dielectric constant with the Zn/ITO ratio. It generally can be noticed that the dielectric constant increased from 6.1 for Zn/ITO = 0.13 to 10.8 for Zn/ITO = 0.55, this can be attributed to the increase of the free carrier concentration with increasing ZnO doping. On the other hand, E_g and ε_i seemed to change in opposite manner as seen from Figs. 5 and 9. This is in agreement with the data obtained by Moss et al. [22].

The substrate deposition temperature was found to have a significant effect on the structure, electrical and optical properties of the ITO films. Figure 10 shows the surface morphology of ZnO doped ITO films with ZnO/ ITO = 0.13 (a_1, a_2, a_3), 0.31 (b_1, b_2, b_3) and 0.55 (c_1, c_2, c_3) at substrate temperatures 100, 150 and 200 °C respectively for each composition. It is clear that, the grains size increase significantly with increasing the deposition substrate temperature from 100 °C to 200 °C.

The optical transmittance curves as a function of the wavelength for the ZnO doped ITO films deposited at various substrate temperatures are shown in Fig. 11. As seen from this figure the transmittance increases with increasing the substrate temperature for all films. This increase in optical transmittance is also related to the increase in grain size of the films with increasing the substrate temperature from 100 °C to 200 °C. It is also observed that the absorption edge shifts towards shorter wavelength, suggesting a widening of the energy band-gap with increasing substrate temperature. This shift in the absorption edge can be explained by the Burstein–Moss effect [23, 24] in which the absorption edge shifts towards higher energy with an increase of carrier concentration [25].

The direct band-gap of the films was calculated from the transmission data in the lower wavelength region using the assumption that the transition probability becomes constant near the absorption edge. The variation of the energy gap as a function of substrate temperature is shown in Fig. 12. One can see from this figure that, the optical energy gap increases with increasing the substrate temperature. According to this increase in the optical band gap, the short wave cutoff wavelength decreased, as shown in Table 1. The basis of the short-wave cutoff wavelength is due to the band gap of the material. It is well known that:

$$\lambda_{\text{cutoff}}\,(\mu\text{m}) = \frac{1.24}{E_g\,(\text{eV})}\,, \tag{6}$$

where E_g is the energy band gap of the material. The cutoff wavelength is directly affected by the energy gap of the material [26]. In the case of ZnO doped ITO thin films deposited at different substrate temperatures, the materials are degenerately doped such that the lowest energy levels of the conduction band are completely filled. This gives an effective band gap larger than that of the intrinsic material. The energy gap is shifted due to the doping of the thin film. The magnitude of the shift is the result of two com-

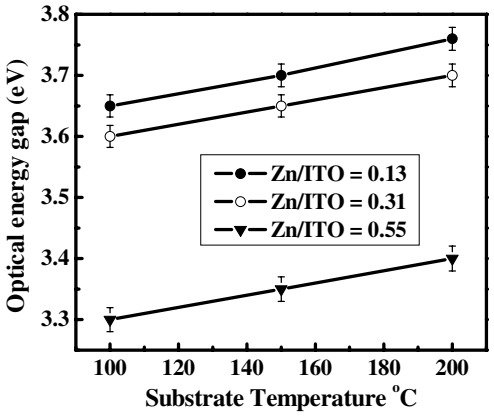

Fig. 12 Variations of the optical band gap E_g with substrate temperatures.

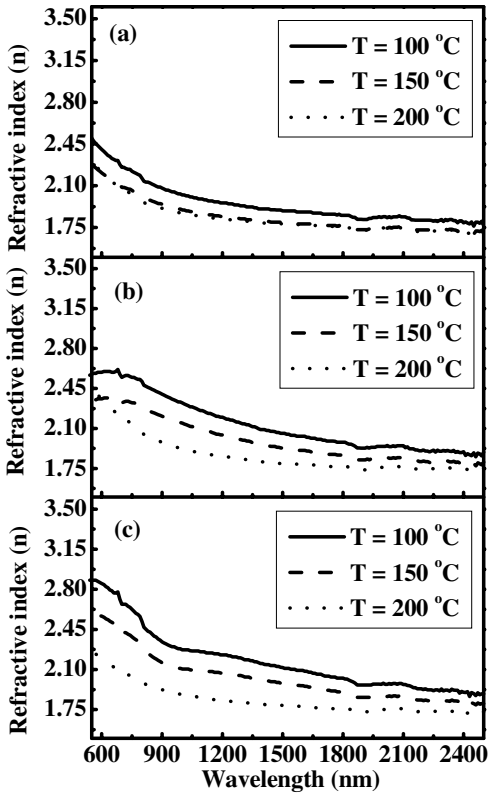

Fig. 13 Wavelength dependence of refractive index of ZnO doped ITO thin films with Zn/ITO = 0.13 (a), 0.31 (b) and 0.55 (c) deposited at different substrate temperature.

peting mechanisms: band gap narrowing due to electron–electron and electron-impurity effects on the valence and conduction bands and band gap widening as a result of the Burstein–Moss effect, a blocking of the lowest states of the conduction band by excess electrons.

Effect of substrate temperature on the electrical resistivity is shown in Table 1. The result shows that the resistivity decreases with the substrate temperature increases, this can be explained by the fact that the grain size increases significantly with increasing the growth temperature, thus reducing the grain boundary scattering and decreasing the resistivity. Values of free carriers concentration and mobility carriers listed in Table 1. It is seen that, the carrier concentration increases with increasing the substrate temperature, thereby reducing the film resistivity.

The refractive index of ZnO doped ITO films deposited at different substrate temperature was calculated from the optical data using Eq. (2). The wavelength dependence of refractive index of the films formed at different substrate temperature is shown in Fig. 13. It is observed that the refractive index of the films is found to increase initially and then decreased with the increase of wavelength. It is clear also that the refractive index of the films is dependent of the substrate temperature. In Table 1, it is also observed that the refractive index (at 550 nm of wavelength) decreases from 2.49 to 2.25 with an increase in the substrate deposition temperature from 100 °C to 200 °C, this can be explained by the increase of the carrier density of the films.

Using the values of refractive index, the long wavelength refractive index (n_∞), average oscillator wave length (λ_o) and oscillator strength S_o for the thin films were determined and listed in Table 1. In order to determine these values, we used the single term Sellmaeir oscillator [27].

The substrate deposition temperature also affects other properties of the film such as the dielectric constant ε_i, the average excitation energy for electronic transitions E_o, the dispersion energy E_d as can see in Table 1.

4 Conclusion

Advancement of TCO's may not only lay within the improvement of existing materials in use (such as SnO_2, ITO, ZnO, etc.), but also the development of novel materials. Zinc oxide doped ITO films of low electrical resistivity ($2.12-12 \times 10^{-3}\ \Omega$ cm) and high visible transmittance (83%) were obtained as a novel TCO material by varying the zinc oxide concentration and substrate temperature. An increase in the band gap (3.23–3.75 eV) was observed by increasing the substrate deposition temperature from 100 to 200 °C. A reduction of the refractive index for ZnO doped ITO films from 2.49 to 2.25 can be achieved by raising the electron density in the films, which can be obtained by increasing the temperature of deposition.

Acknowledgment I would like to thank Prof. Dr. F. M. Elhosary for enabling me to perform the surface morphology of films in his laboratory.

References

[1] R. Jayakrishnan and G. Hodes, Thin Solid Films **440**, 19–25 (2003).
[2] P. K. Biswasa, A. Dea, N. C. Pramanika, P. K. Chakraborty, K. Ortner, V. Hock, and S. Korder, Mater. Lett. **57**, 2326–2332 (2003).
[3] J. C. Manifacier, Thin Solid Films **90**, 297 (1982).
[4] A. Roos, Thin Solid Films **203**, 41 (1991).
[5] G. Sberveglieri, P. Benussi, G. Coccoli, S. Groppelli, and P. Nelli, Thin Solid Films **186**, 349 (1990).
[6] M. A. Matin, A. F. Jezierski, S. A. Bashar, D. E. Lacklison, T. M. Benson, T. S. Cheng, J. S. Roberts, T. E. Sale, J. W. Orton, C. T. Foxon, and A. A. Rezazadeh, Electron. Lett. **30**, 318 (1994).
[7] H. Chen, C. Qiu, M. Wong, and H. S. Kwok, IEEE Electron Device Lett. **24**, 315 (2003).
[8] S.-M. Pan, R.-C. Tu, Y.-M. Fan, R.-C. Yeh, and J.-T. Hsu, IEEE Photonics Technol. Lett. **15**, 649 (2003).
[9] S. J. Chang, M. L. Lee, J. K. Sheu, W. C. Lai, Y. K. Su, C. S. Chang, C. J. Kao, G. C. Chi, and J. M. Tsai, IEEE Electron Device Lett. **24**, 212 (2003).
[10] K. L. Chopra, S. Major, and D. K. Pandya, Thin Film Solids **102**, 1 (1983).
[11] S. M. Rozati and T. Ganj, Renew. Energy **29**, 1671 (2004).
[12] H. Haitjema and J. J. P. Elich, Thin Solid Films **205**, 93 (1991).
[13] M. Tariq Bhatti, A. Manzoor Rana, and Abdul Faheem Khan, Mater. Chem. Phys. **84**, 126 (2004).
[14] P. Manivannan and A. Subrahmanyam, J. Phys. D: Appl. Phys. **26**, 1510 (1993).
[15] H. M. Ali, H. A. Mohamed, and S. H. Mohamed, Eur. Phys. J. Appl. Phys. **31**, 87 (2005).
[16] E. Kh. Shokr, M. M. Wakkad, H. A. Abd El-Ghanny, and H. M. Ali, J. Phys. Chem. Solids **61**, 75 (2000).
[17] X. Wu, T. J. Coutts, and W. P. Mulligan, J. Vac. Sci. Technol. A **15**, 1057–1062 (1997).
[18] F. Wooten, Optical Properties of Solids (Academic Press, San Diego, 1972).
[19] F. Urbach, Phys. Rev. **92**, 1324 (1953).
[20] F. Yakuphanoglu, A. Cukurovali, and I. Yilmaz, Physica B **353**, 210–216 (2004).
[21] S. Wemple, Phys. Rev. B **7**, 3767 (1973).
[22] T. S. Moss, phys. stat. sol. (b) **131**, 415 (1985).
[23] E. Burstein, Phys. Rev. **93**, 632 (1954).
[24] T. S. Moss, Proc. Phys. Soc. Lond. B **67**, 775 (1954).
[25] H. Kim, C. M. Gilmore, A. Piqué, J. S. Horwitz, H. Mattoussi, H. Murata, Z. H. Kafafi, and D. B. Chrisey, J. Appl. Phys. **86**, 6451 (1999).
[26] S. A. Knickerbocker and A. K. Kulkarni, J. Acad. Sci. Technol. A **14**(3), 1709 (1996).
[27] A. K. Wolaton and T. S. Moss, Proc. R. Soc. **81**, 5091 (1963).

